

PARAMETRIC TESTS OF A 40-AH BIPOLAR NICKEL-HYDROGEN BATTERY

Robert L. Cataldo
National Aeronautics and Space Administration
Lewis Research Center
Cleveland, Ohio 44135

ABSTRACT

A series of tests were performed to characterize battery performance relating to certain operating parameters which included charge current, discharge current, temperature and pressure. The parameters were varied to confirm battery design concepts and to determine optimal operating conditions.

INTRODUCTION

Spacecraft power requirements are constantly increasing. Special spacecraft such as the Space Station and platforms will require energy storage systems of 130 kilowatt-hours and 25 kilowatt-hours, respectively. The complexity of these high power systems will demand high reliability, and reduced mass and volume. Candidate electrochemical systems are regenerative fuel cells, nickel-cadmium batteries and nickel-hydrogen batteries.

A system that uses batteries for storage will require a cell count in excess of 400 units. These cell units must then be assembled into several batteries with over 100 cells in a series connected string. In an attempt to simplify the construction of conventional cells and batteries, the NASA Lewis Research Center battery systems group initiated work on a nickel-hydrogen battery in a bipolar configuration in early 1981.

Features of the battery with this bipolar construction show promise in improving both volumetric and gravimetric energy densities as well as thermal management. Bipolar construction allows cooling in closer proximity to the cell components, thus heat removal can be accomplished at a higher rejection temperature than conventional cell designs. Also, higher discharge current densities are achievable because of low cell impedance. Lower cell impedance is achieved via current flow perpendicular to the electrode face, thus reducing voltage drops in the electrode grid and electrode terminal tabs.

BATTERY AND CELL DESIGN

The battery tested was a 12 volt (10 cell), 40 ampere-hour, bipolar battery. The battery was actively cooled with five inter-cell planar cooling plates. The cooling system was operated in the temperature range of 0 degrees centigrade to 40 degrees centigrade; allowing full thermal characterization and determination of appropriate operating temperature.

Accommodations were made for oxygen and electrolyte management. These two functions take place within an electrolyte reservoir plate that contains the oxygen recombination sites. Water, the product of recombination, equilibrates with the electrolyte of the nickel electrode. These functions and other design details are explained in greater depth in a previous paper (Ref. 1).

TEST PROCEDURES

Two initialization cycles were performed prior to characterization. The cycle regime was a C/10 (5.0A.), 13 hour charge and a C/4 (12A.) discharge terminated when the first cell reached 0.5 volts. A value of 50 A-hours was used for the capacity, C, which had been determined from previous tests results. The ampere-hours obtained on discharged the first cycle was 49, and 50 on the second cycle. The results proved that this new battery design could provide the predicted results.

Battery performance was characterized by carrying out a series of parametric tests. Data was obtained at the following conditions: charge rates of C and C/2; discharge rates of 2C, C and C/4; temperatures of 0, 10, 20, 30 and 40 degrees centigrade; base pressures of 200 and 400 pounds per square inch.

Temperatures were maintained by circulating a non-conductive inert fluid through the five cooling plates of the battery. Temperatures were adjusted at static conditions and allowed to stabilize until the inlet and outlet coolant temperatures were equal. The coolant bath temperature was maintained to within 0.1 degrees centigrade by the chiller/heater unit.

The hydrogen pressure was also adjusted at the static discharged condition. The amount of hydrogen generated on charge was small compared to the free volume of the test chamber. Thus, the pressure increase from discharged to full charge was only about 25 pounds per square inch.

TEST RESULTS

Data taken for each charge/discharge cycle was as follows: individual cell voltages, temperatures, ampere-hours and watt-hours. Values were updated and integrated every 18 seconds with a digitizing voltmeter. Both charge and discharge current levels were held constant with power supplies and electronic discharge devices.

Table I and Table II display the test results of ampere-hours, watt-hours and end-of-discharge battery voltage. The remaining battery capacity was drained at the 12 ampere rate (C/4) when the discharge rate was greater than C/4. Charge input was 56 ampere-hours for each test matrix point. The data presented in Table II, 400 psi gas pressure, was a modified matrix where effects of hydrogen gas pressure could be observed at only those conditions

of greatest interest. Table III shows characterization data obtained at all pressure and temperature levels at the same charge rate of two hours and the same 50A (the C rate) discharge. The decision was made to increase the charge input to 65 ampere-hours for this series of tests for two reasons:

- 1) The C/4 drain resulted in total discharge capacities of 54 ampere-hours several times, thereby creating a situation of possible charge deficiency.
- 2) To minimize the influence of varying levels of charge acceptance of the nickel electrode at different temperatures.

Special tests were also conducted to determine battery performance beyond the normally expected range of conventional space power systems. High discharge rates and pulse discharge capabilities were tested because the bipolar battery has exhibited good performance in this area as previously reported (Ref. 2).

The battery was high rate discharged at both constant and pulsed currents for the 250A.(5C) and 500A.(10C) rates to a discharge cutoff voltage of 6.0 volts during the pulse. One additional pulse test was to discharge the battery at 1500A.(30C) for one second where a load voltage of 4.0 volts was established resulting in a 6 kilowatt pulse. This value was lower than expected from previous results (Ref. 2). This lower value of pulse power and the result of a dramatic increase in high rate capacity by pulsing compared to constant discharge level indicated that possibly the area for hydrogen gas access in the frames was not sufficient to support these high discharge rates. This problem was addressed by redesigning the gas access slots in future batteries for pulse applications.

Figure 1 shows plots of the data tabulated in Table 1 and results of the special pulse tests. Figure 1 displays battery voltage and discharge capacity as a function of discharge current at 20 degrees centigrade. The 12, 50 and 100 ampere discharge plots are characteristic of classical battery performance plots. However, the constant load discharge curves of 250 and 500 amperes do not have the standard plateau and knee. This is because of the high rate discharge and possibly the decrease of hydrogen gas concentration at the electrode surface. These two tests were repeated by pulse discharging at a one second on, one second off duty cycle. The off, or relaxation time allows the gas concentration to increase in the gas cavity formed by the hydrogen electrode, gas screen and bipolar plate. The dashed curve in Figure 1 shows the increase in capacity discharged and the increase in watts and watt-hours. The greatest change is noticed of the 250 ampere level where the hydrogen gas concentration depletion is less than that of the 500 ampere rate. An increase in ratio of off to on time may have improved the pulsed performance, particularly at higher rates.

Figure 2 shows the relationship of energy delivered on discharge to battery temperature. The cooling configuration dictates that nickel electrode temperatures were equal over its entire area. A marked increase in energy delivered

and cyclic efficiency was observed at the 30 degree centigrade data point compared to both higher and lower temperatures. At temperatures lower than 30 degrees, battery voltage increases on charge and decreases on discharge causing a net decrease in efficiency. However, above 30 degrees, effects of nickel electrode charging efficiency was seen. These results indicate that a bipolar battery with intercell, planar cooling plates could operate at a higher thermal system temperature than conventional single cell designs that transmit heat in a radial direction via the vessel wall. Therefore, thermal system designs would need to consider the differences in battery design.

Figure 3 shows the battery voltage profile response to pulse discharges of 500 amperes. Only the first four cycles are shown here, although 155 pulses (21.5 ampere-hours) were discharged. The battery voltage drop during the pulse increased from 1.4 volts to 2.2 volts from beginning to end. This increase in voltage drop indicates that a 30 percent change in effective internal cell impedance occurred.

Figure 4 shows the voltage profile for a one pulse maximum power test. A 1500 ampere one second pulse was delivered. Battery voltage, measured at the external terminals of the vessel, was 4.0 volts resulting in a power level of six kilowatts. The instantaneous voltage drop was eight volts for the 1500 ampere pulse. Using these values, a cell resistance of about 0.5 milliohms was calculated.

CONCLUSIONS

The parametric tests conducted on the first actively cooled bipolar nickel-hydrogen battery demonstrates its feasibility. The results are comparable to previous NASA Lewis designs except for its high rate performance. The pulse tests conducted suggest an insufficient gas access to the hydrogen electrode which has resulted in increased polarization. This area has been addressed in other designs for high discharge rates.

The thermal aspects of this battery allow cooling system temperatures of about 30 degrees centigrade for maximum power efficiency. Battery operation in this temperature range of 30 degrees centigrade could have an impact on solar array and radiator sizing.

The NASA Lewis Research Center is working toward establishing a baseline design that would require only simple low cost modifications to the baseline design for integration into various applications. The successful application of active cooling is a major step in developing this baseline design.

REFERENCES

1. R. L. Cataldo, "Design of a 1-kWh Bipolar Nickel-Hydrogen Battery", NASA TM 83647, 1984
2. R. L. Cataldo, "Test Results of a Ten Cell Bipolar Nickel-Hydrogen Battery", NASA TM 83384, 1983

| CR | DR | T | AH(OUT) | WH(IN) | WH(OUT) | EE | EODV |
|-----|-----|----|---------|--------|---------|----|------|
| C | 2C | 0 | 42.4 | 879 | 468 | 53 | 9.3 |
| C | C | 0 | 44.4 | 882 | 533 | 60 | 10.4 |
| C | C/4 | 0 | 49.3 | 883 | 629 | 71 | 10.8 |
| C/2 | 2C | 0 | 43.8 | 845 | 469 | 55 | 8.8 |
| C/2 | C | 0 | 46 | 845 | 545 | 64 | 10.2 |
| C/2 | C/4 | 0 | 51.5 | 851 | 655 | 77 | 10.4 |
| C | 2C | 10 | 43.6 | 856 | 497 | 58 | 9.5 |
| C | C | 10 | 46 | 860 | 557 | 65 | 9.8 |
| C | C/4 | 10 | 51 | 856 | 648 | 75 | 10.1 |
| C/2 | 2C | 10 | 43.5 | 831 | 489 | 59 | 9.3 |
| C/2 | C | 10 | 45 | 834 | 539 | 65 | 9.9 |
| C/2 | C/4 | 10 | 52 | 840 | 656 | 78 | 9.9 |
| C | 2C | 20 | 45.5 | 843 | 529 | 63 | 9.5 |
| C | C | 20 | 47.5 | 842 | 582 | 69 | 10.1 |
| C | C/4 | 20 | 51.5 | 818 | 652 | 80 | 8.4 |
| C/2 | 2C | 20 | 45 | 822 | 524 | 64 | 9.5 |
| C/2 | C | 20 | 48 | 820 | 587 | 72 | 9.7 |
| C/2 | C/4 | 20 | 51.5 | 820 | 655 | 80 | 9.6 |
| C | 2C | 30 | 43 | 834 | 505 | 60 | 10.1 |
| C | C | 30 | 46 | 834 | 560 | 67 | 10.5 |
| C | C/4 | 30 | 50 | 832 | 639 | 77 | 9.5 |
| C/2 | 2C | 30 | 40 | 818 | 470 | 57 | 10.5 |
| C/2 | C | 30 | 44 | 813 | 536 | 66 | 10.4 |
| C/2 | C/4 | 30 | 49 | 818 | 629 | 77 | 9.7 |
| C | C | 40 | 41.8 | 824 | 520 | 63 | 10.6 |
| C/2 | C | 40 | 41.5 | 809 | 516 | 64 | 10.5 |

TABLE I Tabulated test matrix data at 200 psi where:

CR = Charge Rate DR = Discharge Rate T = Temperature
 AH = Ampere-Hours WH = Watt-Hours EE = Energy Efficiency
 EODV = End-Of-Discharge Battery Voltage

| CR | DR | T | AH(OUT) | WH(IN) | WH(OUT) | EE | EODV |
|-----|----|----|---------|--------|---------|------|------|
| C | C | 0 | 37 | 890 | 452 | 51 | 10.9 |
| C/2 | C | 0 | 39 | 857 | 470 | 55 | 10.7 |
| C | C | 10 | 37.8 | 870 | 466 | 53.5 | 11.0 |
| C/2 | C | 10 | 38.5 | 841 | 474 | 56 | 10.8 |
| C | C | 20 | 39.4 | 851 | 490 | 57 | 11.0 |
| C/2 | C | 20 | 39.6 | 829 | 495 | 60 | 10.8 |
| C | C | 30 | 42.2 | 836 | 523 | 62.5 | 9.3 |
| C/2 | C | 30 | 42.2 | 824 | 523 | 63.5 | 9.1 |
| C | C | 40 | 45.5 | 827 | 569 | 69 | 8.7 |
| C/2 | C | 40 | 41.8 | 816 | 521 | 64 | 8.9 |

TABLE II Tabulated test matrix data at 400 psi where:

CR = Charge Rate DR = Discharge Rate T = Temperature
 AH = Ampere-Hours WH = Watt-Hours EE = Energy Efficiency
 EODV = End-Of-Discharge Battery Voltage

| TEMPERATURE °C | PRESSURE (BASE) | AH(OUT) | WH(IN) | WH(OUT) | WATT-HR EFF. | EODV |
|-------------------|--------------------|---------|--------|---------|-----------------|------|
| 0 | 400 | 44 | 1015 | 514 | 51 | 9.7 |
| 10 | 400 | 44 | 1000 | 524 | 52 | 9.9 |
| 20 | 400 | 46 | 978 | 554 | 56.5 | 9.0 |
| 30 | 400 | 48 | 967 | 575 | 60 | 8.9 |
| 40 | 400 | 45 | 980 | 553 | 56.5 | 8.9 |
| 0 | 200 | 43 | 1018 | 502 | 49 | 9.7 |
| 10 | 200 | 42 | 1007 | 502 | 50 | 10 |
| 20 | 200 | 42 | 975 | 506 | 52 | 10.3 |
| 30 | 200 | 44 | 970 | 532 | 55 | 9.8 |
| 40 | 200 | 42 | 957 | 510 | 53 | 8.6 |

TABLE III Characterization Test Matrix
(2 hr. 32.5 ampere charge; C rate (50A.) discharge)

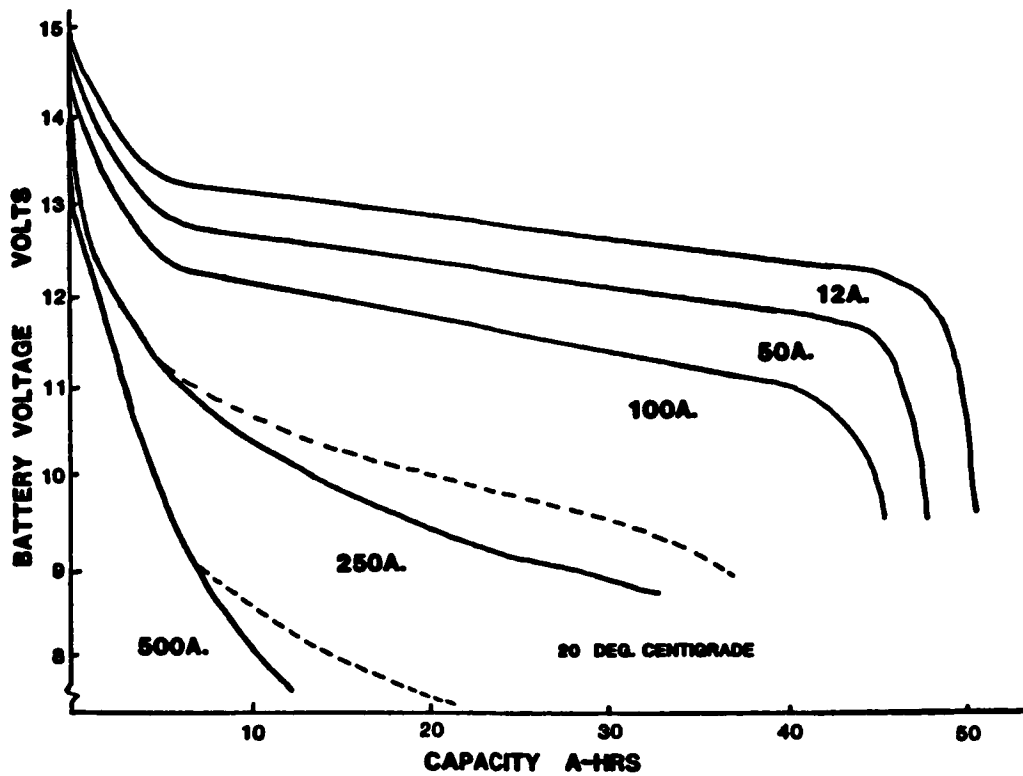


Figure 1. CAPACITY VS. DISCHARGE RATE

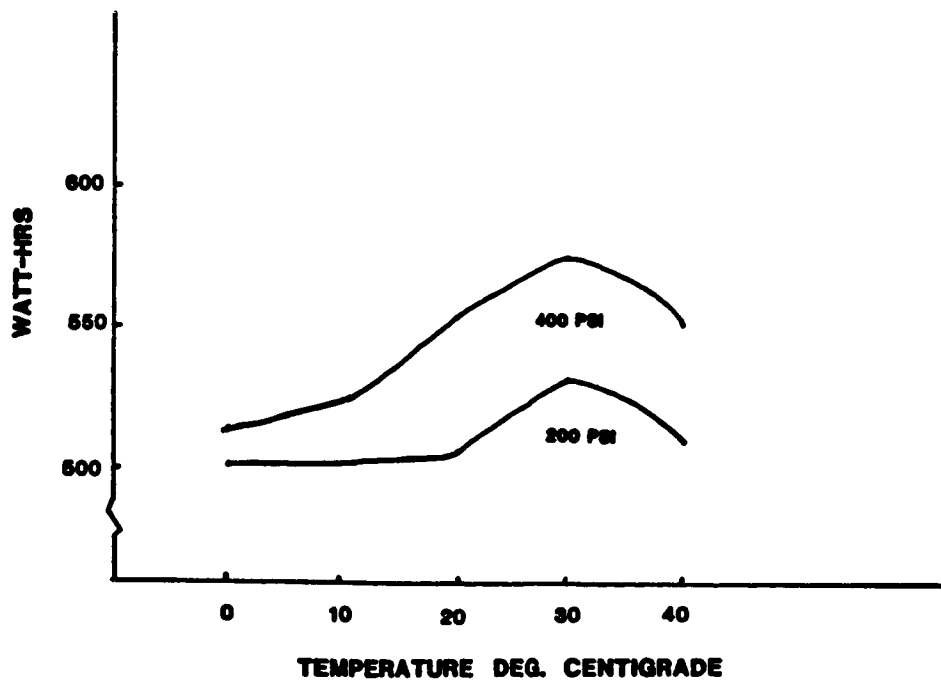


Figure 2. WATT-HRS. VS. TEMPERATURE

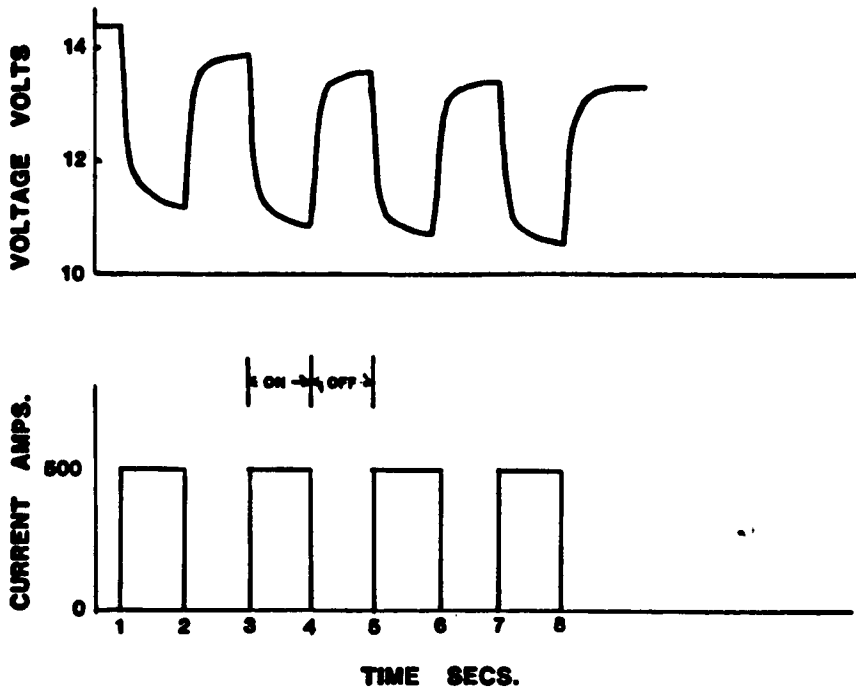


Figure 3. 500 AMPERE PULSE TEST

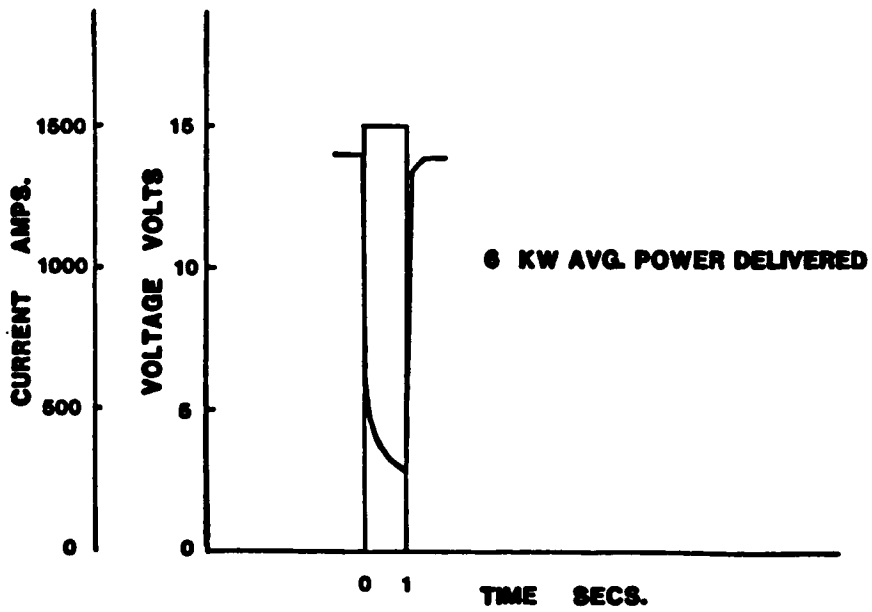


Figure 4. PEAK POWER TEST